# Spin-dependent photoconductivity in hydrogenated amorphous germanium and silicon-germanium alloys

C. F. O. Graeff* and M. Stutzmann†
*Max-Planck-Institut für Festkörperforschung, Heisenbergstrasse 1, D-70569 Stuttgart 80, Germany.*

M. S. Brandt
*Xerox Palo Alto Research Center, Palo Alto, California 94304*
(Received 9 December 1993)

In this work we use spin-dependent photoconductivity (SDPC) to study the recombination process of photoexcited carriers in hydrogenated amorphous germanium (*a*-Ge:H) and silicon germanium alloys (*a*-$Si_xGe_{1-x}$:H). The *a*-Ge:H SDPC signal is found to be strongly affected by the larger spin-orbit coupling, $\lambda$, when compared to *a*-Si:H ($\lambda_{Ge} \approx 7\lambda_{Si}$), which results in a reduced spin-lattice relaxation time. The decrease in the spin-lattice relaxation time gives the following characteristics to the *a*-Ge:H SDPC signal: (i) small amplitudes ($-\Delta\sigma/\sigma \leq 10^{-6}$); (ii) a linear dependence on microwave power, and strong temperature dependence. In *a*-$Si_xGe_{1-x}$:H alloys, the incorporation of Ge is marked by a sudden change in the SDPC signal from Si-like to Ge-like, for $x < 0.9$. The origin of the spin-dependent recombination in *a*-Ge:H and *a*-$Si_xGe_{1-x}$:H is discussed.

## I. INTRODUCTION

Spin-dependent measurements are a convenient method of studying recombination centers.[1,2] In particular spin-dependent photoconductivity (SDPC) has been applied with success to elucidate several processes involved in recombination in *a*-Si:H,[2–7] and to some extent in *a*-$Si_xGe_{1-x}$:H.[8] The great advantage of this technique is that: (1) the measurements can be done at device operation temperatures (around room temperature); (2) the technique is sensitive to the microscopic structure and the chemical environment of paramagnetic defects. Many models have been proposed for the SDPC in *a*-Si:H,[5,9,10] and a natural question that arises is if these models are also valid for other systems. In this work we extend the SDPC technique to *a*-Ge:H and *a*-$Si_xGe_{1-x}$:H. It will be shown that SDPC in *a*-Ge:H is different in origin from the well known case of *a*-Si:H, and a quantitative model describing these differences will be presented.

Hydrogenated amorphous silicon-germanium alloys (*a*-$Si_xGe_{1-x}$:H) have potential applications in devices based on the well established hydrogenated amorphous silicon (*a*-Si:H) technology, but requiring a small-band-gap semiconductor. The most promising application of this material is in different-gap multijunction thin-film solar cells, where higher efficiencies and stability are expected compared to single-junction *a*-Si:H cells.[11,12] Several groups have developed methods to deposit relatively good *a*-$Si_xGe_{1-x}$:H using a variety of feedstocks and preparation conditions.[11–17] However, the optoelectronic quality of *a*-$Si_xGe_{1-x}$:H films in terms of midgap density of states, mobility and carrier lifetime products ($\mu\tau$) of electrons and holes, and conduction band (CB) and valence band (VB) tails are still not sufficient to achieve stable highly efficient multijunction solar cells.[12] The microscopic reason for the decrease of the optoelectronic properties with the germanium (Ge) incorporation is poorly understood.

The incorporation of Ge in *a*-$Si_xGe_{1-x}$:H is found by electron time-of-flight, post-transit spectroscopy and photoconductivity to substantially broaden the CB-tail region close to the CB-mobility edge.[13,14,18] A considerable increase in the number of dangling bonds (DB) with Ge incorporation is also observed.[15,16] On the other hand, the VB tail is little affected by the Ge incorporation.[12–14,18] The alloying effects on the CB-tail are convincingly supported by photoemission spectroscopy measurements,[19] as well as theoretical considerations on the basis of tight-binding calculations, which investigate the consequences of bond length, bond angle, and dihedral angle fluctuations on the electronic density of states of crystalline Si and Ge.[20] It was found that the Si CB edge is affected exclusively by dihedral angle fluctuations, whereas in Ge variations of bond lengths and bond angles additionally affect the electronic density of states at the CB edge. As shown below, SDPC can be used for a detailed study of the recombination process of excess carriers in *a*-$Si_xGe_{1-x}$:H.

## II. EXPERIMENTAL DETAILS

The samples of *a*-$Si_xGe_{1-x}$:H have been prepared either in a conventional parallel plate capacitively coupled glow discharge (GD) reactor, or by cosputtering polycrystalline targets of silicon and germanium. Samples with higher content of germanium were grown by rf sputtering in an atmosphere of argon and hydrogen with a substrate temperature of 200°C. The deposition conditions were those of optimized *a*-Ge:H films.[21] The glow discharge was powered by a dc electric field. Alloying of silicon with germanium was obtained in the GD-deposited samples via different $SiH_4/GeH_4$ gas mixtures diluted with

 

$H_2$. Gas pressure (0.3 mbar) and substrate temperature (200 °C) were held constant for all deposition runs. Further details about deposition conditions and sample properties are given in Refs. 14 and 17.

Standard techniques have been employed in order to characterize the specimens. Optical transmission measurements between 500 and 2000 nm were used for the determination of film thickness, optical band gap, and refractive index. The Fermi level position was obtained from measurements of the temperature-dependent dark conductivity ($300 < T < 450$ K). The composition of the films was determined via the optical gap, and in some cases by electron microprobe analysis.

The SDPC technique detects spin resonance by changes in the steady-state photoconductivity.[2–7,22] For the SDPC experiments, we used $a$-$Si_xGe_{1-x}$:H thin films grown on Corning 7059 glass, with interdigit coplanar Al electrodes. The samples were illuminated by a heat-filtered tungsten lamp ($\approx 60\,\mathrm{mW/cm^2}$) and were kept at a constant temperature ($100 < T < 300$ K) by cooling with dry nitrogen. The samples were placed in the $TE_{102}$ cavity of a standard $X$-band electron paramagnetic resonance (EPR) spectrometer (BRUKER ESP 300). The spin-dependent change of the photoconductivity is especially small for $a$-Ge:H and $a$-$Si_xGe_{1-x}$:H (typically $\Delta\sigma/\sigma \leq 10^{-6}$). In order to obtain a sufficient signal-to-noise ratio, modulation of the static magnetic field ($H_0$) together with lock-in detection was necessary.

## III. THEORETICAL APPROACH

In this section a brief revision of previous theoretical work is presented. In addition, a phenomenological theory for the resonant change in $a$-Ge:H is developed.

The SDPC signal is related basically to an increase in the recombination rate when the spin system is brought into resonance. This increase in the recombination rate comes from the implications of spin conservation: if the spin-orbit interaction is not large, recombination transitions will conserve total spin. For recombination processes involving one or both trapped carriers, the final state is in general a singlet ($S = 0$). This is the case considered in this study, where the main recombination channel in $a$-Si:H and $a$-Ge:H is the nonradiative capture of an electron in a CB-tail state by a hole in a DB state. From the above consideration the triplet state recombination is forbidden. A resonant microwave field induces spin flips of either the electron or hole and, thus, promotes a redistribution of spin states. This will in turn produce a change in recombination rate.

Using the terminology of Movaghar, Ries, and Schweitzer,[10] the microwave-induced transitions that give rise to an increase in the recombination rate can be basically of two types: anomalously spin dependent and normally spin dependent. What distinguishes the two is the relation between the various characteristic time constants involved in the process: the spin-lattice relaxation time $T_1$, the recombination lifetime $\tau$, and the thermal emission time.

### A. Anomalously spin-dependent photoconductivity ($a$-Si:H case)

Normally spin-dependent recombination was the first model developed for SDPC.[22] However, the signal amplitudes measured either in $c$-Si,[22] or $a$-Si:H,[2–5] are orders of magnitude larger than the predictions using this model. Therefore, the SDPC signal in $a$-Si:H is anomalously spin dependent. The important feature in this latter approach is the long lifetime of the spin states prior to the recombination. To obtain an anomalous spin dependence, the relaxation times $T_1$ for both spins involved in the recombination must be long compared to the transition times (recombination, or reemission to the conduction path) of spin-allowed transitions. Before recombination, the spins thermalize randomly into singlet ($S = 0$) and triplet ($S = 1$) pair states. But since only singlet recombination is allowed from spin selection rules, an excess of long-lived triplet states is built up. Spin resonance transfers these triplet pairs into singlets, thus increasing the recombination probability. Although an exact quantitative analysis of the experimental data is difficult using this model, Kaplan *et al.*[9] have made quite good estimations of anomalous SDPC signal amplitudes with simple approximations. Since this SDPC model does not apply to $a$-Ge:H or $a$-$Si_xGe_{1-x}$:H, we refer to previously published work for further details.[9,10]

### B. Normally spin-dependent photoconductivity ($a$-Ge:H case)

The second kind of transition (normally spin dependent), occurs if at least one of the carriers (electron or hole) has a spin relaxation time shorter than the recombination lifetime of a singlet pair. In this case the spin coherence time is short, and no long-lived pairs are formed.

In the normally spin-dependent case, as derived by Lépine,[22] the capture cross section of the CB electrons by the recombination center is supposed to be dependent on the relative orientations of their spins. Triplet or singlet collisions of the CB electron on the recombination centers (parallel or antiparallel spins) give rise to triplet or singlet final states for the system CB electron plus recombination center. In this simple approach, triplet states do not recombine at all, while singlet states are allowed to recombine. The capture cross section $\Sigma$ for the CB electron therefore should have the following form:

$$\Sigma = \Sigma_0 (1 - \pi\Pi) \quad , \tag{1}$$

where $\pi$ and $\Pi$ are the spin polarizations of the CB and recombination centers, respectively. The recombination time $\tau$ is a function of $\Sigma$ and, in the simplest case, a relative variation of $\Sigma$ will result in an equal and opposite variation of $\tau$: $\delta\tau/\tau = -\delta\Sigma/\Sigma$. From Eq. (1) a change in $\pi$ and/or $\Pi$ will induce a change in $\Sigma$ and consequently in $\tau$. The departure from the unpolarized state ($\Pi = 0$) is

induced by the dc magnetic field $H_0$ used to produce the Zeeman splitting of the spin level. The resonant microwave field induces transitions between the Zeeman spin levels and tends to equalize their populations, or in other words tends to destroy the magnetic-field-induced polarization. Hence the spin polarization of the system is reduced and, in the limit of infinite microwave power, vanishes.

The effect of a reduction of $\tau$ is observed as a decrease in the photoconductivity $\sigma = ne\mu$, where $e$ is the electron charge, $\mu$ the electron mobility, and $n$ is the excess carrier concentration. Remembering that for monomolecular recombination $n \approx G\tau$ ($G$ is the generation rate), in this case the change in the photoconductivity is $\delta\sigma/\sigma = \delta\tau/\tau$. Differentiating Eq. (1), and using the relation that $\pi, \Pi \ll 1$, one obtains

$$-\frac{\delta\sigma}{\sigma} = \frac{\delta\Sigma}{\Sigma} = -\delta(\pi\Pi). \tag{2}$$

The polarization is defined as $\pi = \pi_+ - \pi_-$, where $\pi_+$ and $\pi_-$ are the population fractions of the two Zeeman levels ($\pi_+ + \pi_- = 1$). Since the spins are in equilibrium with the lattice prior to the application of the resonant microwave field, the thermal equilibrium ratio $(\pi_+/\pi_-)$ is $\exp(\gamma\hbar H_0/kT)$. In the high-temperature approximation the equilibrium polarization can be written as

$$\pi_0 = \frac{\gamma\hbar H_0}{2kT}. \tag{3}$$

At room temperature and a field of 3300 G, $\pi_0 \approx 10^{-6}$. When the microwave field is on, the value of $\pi$ is determined by the competition of the resonant rf field that tends to saturate the electron spin resonance (ESR) (making $\pi = 0$) with the spin-lattice relaxation that tends to restore equilibrium (making $\pi = \pi_0$). In this case, making use of the transition probability method, $\pi$ under resonance is[23]

$$\pi = \pi_0 \left\{ 1 - \frac{\omega_1^2 T_1^2}{\omega_1^2 T_1^2 + 1} \right\}, \tag{4}$$

for a homogeneously broadened Lorentzian line. $\omega_1 = \gamma H_1$ is the microwave-induced spin-flip rate. For an inhomogeneously broadened line, where the distribution of Larmor frequencies is much broader than $\omega_1$ and $1/T_1$, one obtains

$$\pi = \pi_0 \left\{ 1 - \frac{\omega_1^2 T_1^2}{\sqrt{\omega_1^2 T_1^2 + 1}} \right\}, \quad \omega_1 T_1 < 1. \tag{5}$$

In the two previous equations, we are assuming that the spin-spin relaxation time $T_2$ is always longer than $T_1$, and thus $T_2$ is limited by $T_1$, or $T_2 = T_1$. As an example, we calculate the SDPC signal amplitude ($-\delta\sigma/\sigma$, or $-\Delta\sigma/\sigma$, since the changes are always much smaller than 1) for a hypothetical homogeneously broadened Lorentzian line in $a$-Ge:H. There, $T_1$ for the CB-tail electrons is much smaller than the $T_1$ of the DB in the temperature range used (100–300 K).[24] In this case, $\delta\pi\Pi \approx \pi_0\delta\Pi \approx \pi_0(\Pi - \Pi_0)$. Thus Eq. (2) gives

$$-\frac{\Delta\sigma}{\sigma} = \pi_0\Pi_0 \frac{\omega_1^2 T_1^2}{\omega_1^2 T_1^2 + 1} = \left(\frac{\gamma\hbar H_0}{2kT}\right)^2 \frac{\omega_1^2 T_1^2}{\omega_1^2 T_1^2 + 1}. \tag{6}$$

## IV. RESULTS AND DISCUSSION

SDPC has been successfully used for understanding details of the recombination process in $a$-Si:H.[2–7] The recombination process in $a$-$Si_xGe_{1-x}$:H (and alloys in general) is more complex than in elemental amorphous semiconductors, since both Si and Ge atomic orbitals are involved in the formation of DB's, CB, and VB states. Before treating the more intricate problem of the alloys let us first deal with the simpler case of $a$-Ge:H.

### A. Spin-dependent photoconductivity in $a$-Ge:H

Although similar in many respects, $a$-Ge:H and $a$-Si:H differ appreciably in what concerns their spin properties. Of particular interest here is the fact that Ge has a larger atomic spin-orbit coupling constant than Si ($\lambda_{Si} = 0.019$ eV, $\lambda_{Ge} = 0.138$ eV). As the spin-lattice relaxation time $T_1$ in $a$-Ge:H and $a$-Si:H is determined by the spin-orbit coupling and therefore is proportional to $\lambda^{-2}$, a two orders of magnitude smaller relaxation time results in $a$-Ge:H when compared to $a$-Si:H.[24] One immediate consequence of this smaller $T_1$ is that for the microwave powers normally used in SDPC experiments (10–400 mW), unlike $a$-Si:H, the spin system of $a$-Ge:H is not in the saturation regime. In a phenomenological treatment of relaxation based on the Bloch equation, saturation occurs when the precessional frequency of the spins $\gamma H_1$ ($\gamma$ is the gyromagnetic ratio, and $H_1$ is the rotating component of the microwave magnetic field inducing transitions), becomes greater than the corresponding relaxation frequencies, $1/T_1$, or, more precisely, when the saturation parameter $S$ ($S = \gamma^2 H_1^2 T_1 T_2$, where $T_2$ is the spin-spin relaxation time) is larger than 1.[25]

We mention in passing a problem when comparing SDPC signal amplitudes for signals with largely varying peak-to-peak linewidths, $\Delta H_{pp}$. Strictly speaking, the entire effect of spin resonance on the conductivity is obtained by performing a double integration over the derivative signal, as in standard spin density measurements. The amplitude of the SDPC signal is thus related to the total spin dependence by a factor $(\Delta H_{pp}/H_{mod})^2$, where $\Delta H_{pp}$ is the peak-to-peak linewidth and $H_{mod}$ the modulation amplitude. When comparing SDPC results of materials with largely different linewidths such as $a$-Si:H and $a$-Ge:H, care has to be taken to correctly account for the differences in $\Delta H_{pp}$, either by including the above correction, or by using a modulation amplitude $H_{mod}$ close to $\Delta H_{pp}$ in all cases. In our experiment

we used the latter condition, so that the SDPC signal amplitudes can be compared directly.

We start by recalling the definition of the dynamic susceptibility $\chi = \chi' + i\chi''$ for the response of a spin system to an external resonant microwave field $H_1$. For a homogeneous line we have for the imaginary part:

$$\chi'' = \frac{1}{2}\chi_0\omega_0 \frac{T_2}{1+\gamma^2 H_1^2 T_2 T_1}, \tag{7}$$

whereas for an inhomogeneous line:

$$\chi'' = \frac{1}{2}\chi_0\omega_0 \frac{h(\omega-\omega_0)}{(1+\gamma^2 H_1^2 T_2 T_1)^{\frac{1}{2}}}, \tag{8}$$

where $\chi_0$ is the static susceptibility $\omega_0 = \gamma H_0$, and $h(\omega-\omega_0)$ is the distribution of static fields that give origin to the inhomogeneous line. The ESR signal of our spectrometer uses the linear region of a diode detector, and thus is proportional to the square root of the microwave power (or proportional to the out-of-phase component of the magnetization $M_y = \chi'' H_1$).[26] In this case the relative signal measured by the spectrometer has the form[27]

$$V_{\mathrm{ESR}} = \frac{\sqrt{S}}{1+S} \tag{9}$$

for a homogeneously broadened line, and the form

$$V_{\mathrm{ESR}} = \sqrt{\frac{S}{1+S}} \tag{10}$$

for a completely inhomogeneously broadened line. This is shown by the dashed curves in Fig. 1(a).

The SDPC signal, on the other hand, is proportional to the microwave-induced spin-flip rate, or the microwave power absorbed $\chi'' H_1^2$. Thus we expect for experimental conditions where this proportionality is correct that the SDPC signal behaves as

$$V_{\mathrm{SDPC}} \propto V_{\mathrm{ESR}} H_1 \propto V_{\mathrm{ESR}}\sqrt{P}, \tag{11}$$

where $P$ is the microwave power. Thus, plotting $V_{\mathrm{SDPC}}/\sqrt{P}$ versus microwave power should yield the same saturation behavior as for the ESR signal. This is demonstrated in Fig. 1(b) for the case of $a$-Si:H: for low microwave powers (unsaturated regime) $V_{\mathrm{SDPC}}/\sqrt{P} \propto \sqrt{P}$ (in other words $V_{\mathrm{SDPC}}$ is proportional to the microwave power), whereas in saturation $V_{\mathrm{SDPC}}/\sqrt{P} \approx$ constant (i.e., $V_{\mathrm{SDPC}} \propto \sqrt{P}$), since the $a$-Si:H resonance is inhomogeneous. In our experiments, the onset of saturation (marked by the transition from $P$ to $\sqrt{P}$ dependence) occurs at microwave powers of typically 1 mW. This is also observed in the ESR saturation power for Si dangling bonds at 300 K, shown as filled circles in Fig. 1(a).

In the case of $a$-Ge:H, however, the much shorter $T_1$ [$T_1$($a$-Si:H) $\geq$ 100$T_1$($a$-Ge:H)] causes the saturation to occur at a much higher microwave power ($\approx$ 10 W), so that the $a$-Ge:H SDPC response should always be proportional to $P$. This is in agreement with experimental data in Fig. 1(b). Note that this behavior is also expected from Eq. (6). Note also the two orders of magnitude smaller signal amplitude found in $a$-Ge:H when compared to $a$-Si:H.

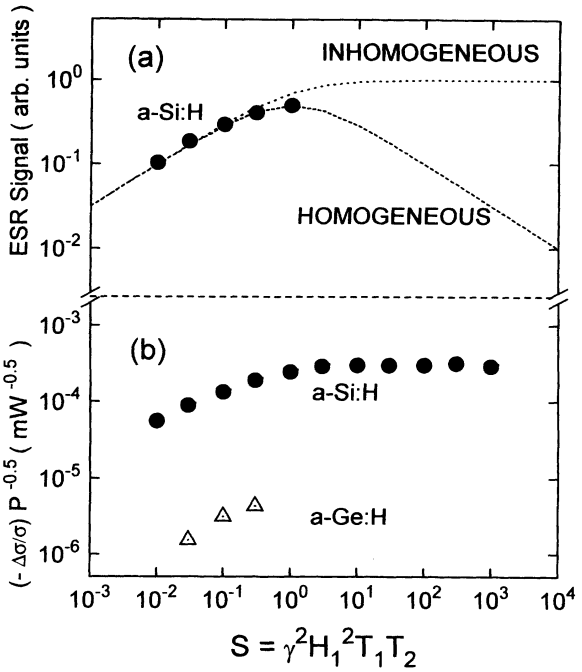


FIG. 1. (a) Calculated normalized ESR signal for a homogeneously and inhomogeneously broadened line as a function of the saturation parameter $S$. In the same figure, dots represent experimentally observed ESR signals from $a$-Si:H. (b) SDPC signal $(-\Delta\sigma/\sigma)$ divided by the square root of the microwave power ($P$) against the saturation parameter $S$, for $a$-Si:H (filled circles) and $a$-Ge:H (open triangles).

The smaller $T_1$ in $a$-Ge:H is responsible for the change from anomalous (in $a$-Si:H) to normal (in $a$-Ge:H) spin-dependent transport, as seen in Fig. 2, where the temperature dependence of the SDPC signal for $a$-Ge:H and $a$-Si:H is shown. In the same figure the predicted values for $(-\Delta\sigma/\sigma)$ using Eq. (6) are shown as a dashed line, where we have used the temperature dependence of $T_1$, $T_1 \propto T^{-2}$.[24] Also plotted as the dotted line is the maximum predicted change for $(-\Delta\sigma/\sigma)$, assuming an infinite microwave power ($\omega_1 T_1 \gg 1$). As can be seen, the $a$-Ge:H data are in good agreement with the proposed model Eq. (6). We have assumed for simplicity that the SDPC signal line shape is homogeneously broadened. No significant change is to be observed if Eq. (5) is used instead of Eq. (4) when deriving Eq. (6). Note that for $a$-Si:H, as expected, the SDPC signal amplitude is orders of magnitude larger than the maximum predicted value, using the normally spin-dependent model. Note also that no appreciable change with temperature is observed in the $a$-Si:H SDPC signal.

Summarizing, due to the larger spin-orbit coupling and consequently smaller spin-lattice relaxation times, the SDPC signal of $a$-Ge:H, when measured in the same con-

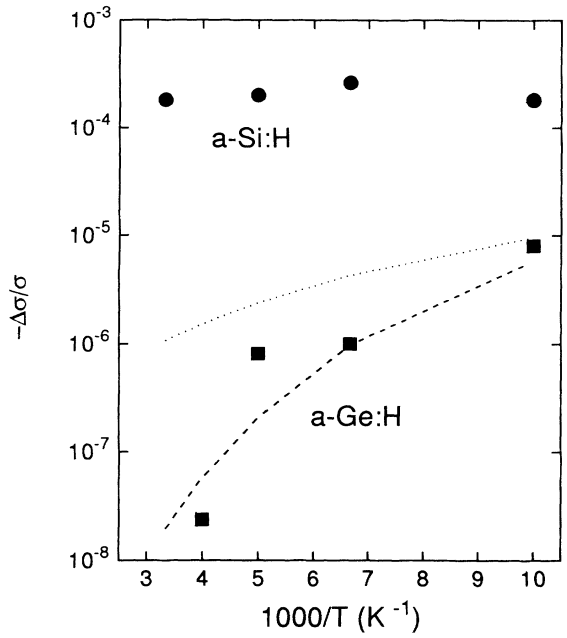


FIG. 2. SDPC signal ($-\Delta\sigma/\sigma$) vs the inverse temperature for $a$-Si:H and $a$-Ge:H. The dotted line is the calculated upper limit for the SDPC signal in the normally spin-dependent model. The dashed line represents the calculated amplitude using Eq. (6), i.e., including the temperature dependence of the spin-lattice relaxation.

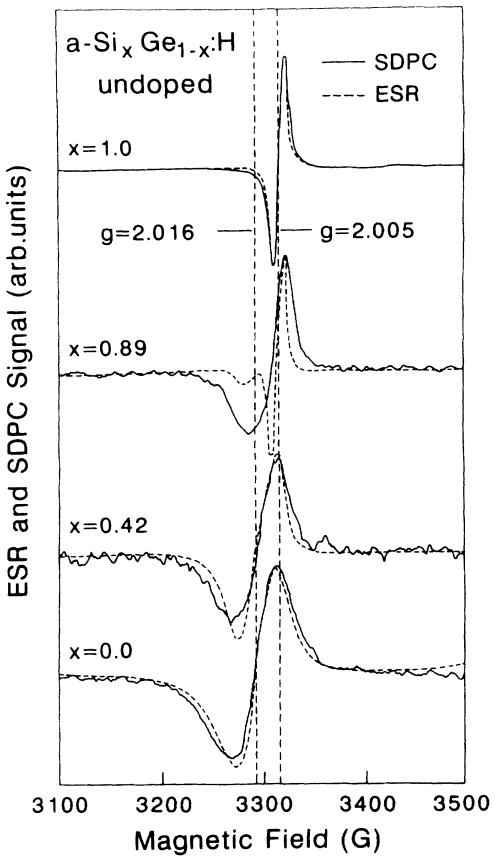


FIG. 3. ESR (dashed lines) and SDPC (full lines) signal as a function of the external magnetic field, for alloys with different composition. The characteristic $g$ values of the $a$-Si:H (2.005) and $a$-Ge:H (2.016) SDPC signals are shown as vertical lines.

ditions as $a$-Si:H, has the following characteristics.

(i) A stronger dependence on incident microwave power, $-\Delta\sigma/\sigma(\mathrm{Ge}) \propto P$, versus $-\Delta\sigma/\sigma(\mathrm{Si}) \propto P^{1/2}$ The two dependencies follow from the fact that the spin system of $a$-Si:H is in saturation, while in $a$-Ge:H it is not.

(ii) A smaller absorption amplitude $\{-\Delta\sigma/\sigma(\mathrm{Si}) \geq 100[-\Delta\sigma/\sigma(\mathrm{Ge})]\}$, and a strong temperature dependence. These two effects are understood using Movaghar *et al.*'s[10] description of SDPC. $a$-Ge:H has a normally spin-dependent recombination process, while in $a$-Si:H the recombination is anomalously spin dependent.

### B. Spin-dependent photoconductivity in $a$-$Si_xGe_{1-x}$:H

In the previous section we confined our discussion to the elemental semiconductors that compose $a$-$Si_xGe_{1-x}$:H, giving special emphasis to $a$-Ge:H. Let us treat now the more intricate problem of the $a$-$Si_xGe_{1-x}$ :H alloy case.

In Fig. 3 we summarize typical SDPC spectra for the alloys, as a function of composition (full lines). In the same figure the corresponding spectra of conventional ESR on similar samples are presented (dashed lines). It is clear from the figure that the two techniques give quite different line shapes, especially in the Si-rich alloys. Thus the incorporation of Ge has a more pronounced effect on SDPC than on ESR spectra. The different line shapes reflect the different origin of the SDPC and ESR signals. ESR in these materials measures the Si and the Ge DB density.[15,16,28] This is particularly visible in the $x = 0.89$ case, where the components coming from the Si and Ge DB's are easily deconvoluted. The SDPC signal is more complex in nature. The SDPC signal is not just sensitive to the densities of DB, CB, or VB states but also to the main process of recombination. The deconvolution of all these contributions to the SDPC signal is a rather involved problem.

The elemental semiconductors ($a$-Si:H and $a$-Ge:H) give similar line shapes for SDPC and ESR spectra, although the SDPC signal is broadened, and has a $g$ factor between the ESR $g$ factors for an electron in a DB and in the CB tail states. For example, in undoped $a$-Ge:H the $g$ value found in SDPC is $\approx 2.016$, between 2.018 (Ge DB) and 2.012 (Ge CB tail).[28] The $g$ factor found in $a$-Ge:H SDPC, as in $a$-Si:H,[2–5] indicates that the main recombination process is of an electron in the CB tail being captured by a hole in a DB. In the alloys, on the other hand, ESR and SDPC spectra are remarkably different. Note that for $x = 0.89$ the SDPC signal line shape is mainly Ge-like. This is clear evidence for a strong participation of Ge in the recombination process. Not just the line shape is Ge-like, but also the signal magnitude. In Fig. 4 the SDPC signal against the incident microwave power is shown for various alloy compositions. Again, as

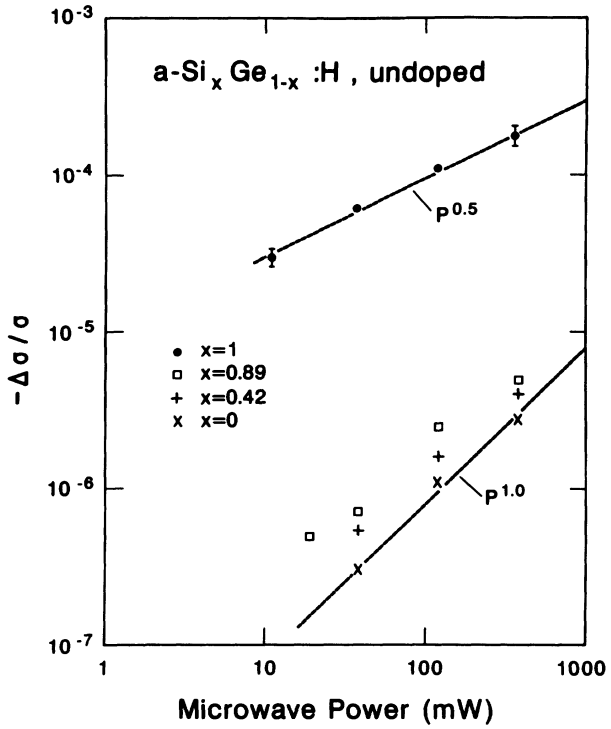


FIG. 4. SDPC signal $(-\Delta\sigma/\sigma)$ as a function of incident microwave power in mW for various alloy compositions. Note that even for the Si-rich alloys ($x = 0.89$) the SDPC signal is similar to that in pure Ge.

soon as Ge is incorporated ($x = 0.89$), the SDPC signal amplitude and power dependence become similar to those in $a$-Ge:H.

The origin of the Ge-like behavior of the SDPC signal in $a$-$Si_xGe_{1-x}$:H, assuming a homogeneous material, can be either a higher number and/or larger capture cross section of Ge DB's, or a strong modification of the CB tail due to alloying. As already mentioned, there is independent evidence that the incorporation of germanium in $a$-$Si_xGe_{1-x}$:H has a strong effect on the distribution of localized states just below the CB mobility edge. Let us start from this possibility, which seems physically more reasonable to us. Assuming that the CB-tail states are Ge-like (Ge-Ge antibonding states), a decrease in the spin relaxation time of the electrons occupying these states is expected. This implies a transition from anomalous to normal spin-dependent recombination, as discussed in Sec. II, and observed in Fig. 4. The asymmetry of the SDPC line shape for small Ge concentrations can also be understood in the context of this model. A broad asymmetric line should occur, if an electron occupying a Ge CB-tail state recombines with a hole in a Si DB. Going further with this assumption, to deconvolute the SDPC signal, it is assumed that the measured $g$ factor in the alloys, as in the case of $a$-Si:H and $a$-Ge:H, is an average between the $g$ factors of electrons occupying a DB and CB-tail state. Due to the asymmetry in the line shape of the SDPC spectra in $a$-$Si_xGe_{1-x}$:H (see Fig. 3), the $g$ factor was calculated using the following equation:[29]

$$\tilde{g} = \frac{\int g(H)S(H)dH}{\int S(H)dH} = \frac{g_{CB} + g_{DB}}{2}. \quad (12)$$

where $S(H)$ is the SDPC absorption shape as a function of the static magnetic field $H$, which is obtained by integrating the derivative SDPC signal. Since the DB state can be from either Si or Ge, in our calculation we have used the $g$ factors for the DB ($g_{DB}$) presented in Ref. 29, that were obtained theoretically and experimentally for the whole alloy range. In this case, the CB-tail contribution to $\tilde{g}$ is simply $g_{CB} = 2\tilde{g} - g_{DB}$. The $g_{CB}$ obtained by this procedure as a function of alloy composition are presented in Table I. Note that the CB-tail $g$ value is very similar to the one found in $n$-type doped $a$-Ge:H,[16,28] confirming the hypothesis that the Ge incorporation is followed by the creation of Ge-like states in the CB tail. These new states act as traps for the excited electrons, prior to recombination.

To discuss the other possibility, namely, that the Ge DB's are the dominant path for recombination, let us treat the $x = 0.89$ case as an example. For this alloy, to a good approximation, the density of Ge and Si DB's are the same and equal to $10^{16}$–$10^{17}$ $cm^{-3}$. For a randomly mixed alloy, the average distance between the DB's is then 200 Å or more. At this distance a negligible overlap between the DB wave functions is expected. Assuming that the CB-tail is Si-like (unperturbed), an electron that recombines into a Si DB will be anomalously spin dependent, while an electron recombining into a Ge DB will be normally spin dependent, as discussed above. Thus the recombination into Si DB's would give a SDPC signal amplitude at least 100 times greater than recombination via a Ge DB (see Fig. 4). In this case, in order to explain the observed Ge-like features of the SDPC signal, one would have to assume that the Ge DB capture cross section is about three orders of magnitude larger than that of a Si DB. This assumption is at variance with previous results using optically detected magnetic resonance (ODMR), which indicated that the Si DB plays the dominant role in recombination in the whole alloy range.[15] This assumption is also in contradiction to published experimental results, which indicate that the capture cross sections of Si DB's and Ge DB's are basically the same, independent of alloy composition.[30] Thus, the SDPC data for the alloys indicate that even for small Ge concentrations the conduction band tail becomes Ge-like.

Before concluding we would like to mention that recently Paul *et al.*[12] pointed out that another possibil-

TABLE I. Estimated and observed $g$ factors for paramagnetic defects in $a$-$Si_xGe_{1-x}$:H, using SDPC. $g_{DB}$ was obtained from Ref. 29, $\tilde{g}$ is the measured $g$ value, and $g_{CB}$ is the derived $g$ factor for the electron in the conduction band.

| Composition $x$ | $g_{DB}$ | $\tilde{g}$ | $g_{CB}$ |
|---|---|---|---|
| 1.0 | 2.0055 | 2.0048 | 2.0041 |
| 0.9 | 2.008 | 2.011 | 2.014 |
| 0.7 | 2.015 | 2.013 | 2.011 |
| 0.5 | 2.017 | 2.014 | 2.012 |
| 0.0 | 2.020 | 2.017 | 2.014 |

ity for the decrease in electron mobility is the presence of long-range potential fluctuations (LRPF's) in the alloys. In the LRPF model the lowest-energy CB states, which could arise from a Ge-rich region for example, act as scattering centers for the electrons. In this way, the presence of LRPF's increases the number of scattering centers, consequently decreasing the mobility of the carriers. If LRPF is the dominant effect responsible for the decrease in the electron mobility, in opposition to the assumed homogeneity of the material in the analysis made before, the results presented here indicate that the dominant scattering centers (lower-energy states of the CB tail) for electrons as expected are Ge-like states.

## V. CONCLUSIONS

We have found that the SDPC signal in $a$-Ge:H is fundamentally influenced by the large atomic spin-orbit coupling of Ge and the resulting shorter spin relaxation time. The SDPC signal of $a$-Ge:H can be quantitatively modeled as originating from magnetic field polarization effects on the spin system.

SDPC results in $a$-$Si_xGe_{1-x}$:H indicate that the Ge incorporation in the $a$-Si:H network creates Ge-like states in the CB tail. These states dominate the transport and recombination of the photoexcited carriers in the whole alloy range covered in this study ($0.1 < x < 0.89$).

## ACKNOWLEDGMENTS

We would like to thank K. Eberhardt from the University of Stuttgart for sample preparation. C. F. O. Graeff acknowledges support from CAPES/DAAD and FAPESP. This work was supported by the Bundesminister für Forschung und Technologie under Contract No. 0328962A.

* Present address: Instituto de Física "Gleb Wataghin", Unicamp, 13081-970 Campinas, Brazil.
† Permanent address: Walter Schottky Institut, Technische Universität München, Am Coulombwall, 85478 Garching, Germany.

[1] B.C. Cavenett, Adv. Phys. **30**, 475 (1981).
[2] K. Lips, S. Schütte, and W. Fuhs, Philos. Mag. B **65**, 945 (1992).
[3] I. Solomon, D.K. Biegelsen, and J.C. Knights, Solid State Commun. **22**, 505 (1977).
[4] R.A. Street, Philos. Mag. B **46**, 273 (1982).
[5] H. Dersch, L. Schweitzer, and J. Stuke, Phys. Rev. B **28**, 4678 (1983).
[6] M.S. Brandt and M. Stutzmann, Phys. Rev. B **43**, 5184 (1991).
[7] M. Stutzmann and M.S. Brandt, J. Non-Cryst. Solids **141**, 97 (1992).
[8] C.F.O. Graeff, M.S. Brandt, K. Eberhardt, I. Chambouleyron, M. Stutzmann, J. Non-Cryst. Solids **164-166**, 15 (1993).
[9] D. Kaplan, I. Solomon, and N.F. Mott, J. Phys. (Paris) **39**, L51 (1978).
[10] B. Movaghar, B. Ries, and L. Schweitzer, Philos. Mag. B **41**, 141 (1980); **41**, 159 (1980).
[11] D.E. Carlson, IEEE Trans. Electron Devices **36**, 12 (1989).
[12] W. Paul, R.A. Street, and S. Wagner, J. Electron. Mater. **22**, 39 (1993).
[13] S. Aljishi, Z. Smith, and S. Wagner, in *Amorphous Silicon and Related Materials*, edited by H. Fritzsche (World Scientific, Singapore, 1988), p. 887.
[14] C.E. Nebel, M. Schubert, H.C. Weller, G.H. Bauer, and W.H. Bloss, in *Proceedings of the 8th EC Photovoltaic Solar Energy Conference*, edited by I. Solomon, B. Equer, and P. Helm (Reidel, Dordrecht, 1988), p. 919.
[15] W. Fuhs and F. Finger, J. Non-Cryst. Solids **114**, 387 (1989).
[16] M. Stutzmann, R.A. Street, C.C. Tsai, J.B. Boyce, and S.E. Ready, J. Appl. Phys. **66**, 569 (1989).
[17] H.C. Weller and G.H. Bauer, in *Amorphous Silicon Technology—1989*, edited by A. Madan, M.J. Thompson, P.C. Taylor, Y. Hamakawa, and P.G. LeComber, MRS Symposia Proceedings No. 149 (Materials Research Society, Pittsburgh, 1989), p. 339.
[18] F. Karg, W. Krühler, M. Möller, and K.v. Klitzing, J. Appl. Phys. **60**, 2016 (1986).
[19] F. Evangelisti, J. Non-Cryst. Solids **77&78**, 969 (1985).
[20] K. Tanaka and R. Tsu, Phys. Rev. B **24**, 2083 (1981).
[21] C.F. de O. Graeff, P.V. Santos, G. Marcano, and I. Chambouleyron, in *Proceedings of the 21st IEEE Photovoltaic Specialist Conference* (IEEE, New York, 1990), p. 1564.
[22] D. Lépine, Phys. Rev. B **6**, 436 (1972).
[23] A. Abragam, *Principles of Nuclear Magnetism* (Oxford University Press, Oxford, 1961), p. 31.
[24] M. Stutzmann and D.K. Biegelsen, Phys. Rev. B **28**, 6256 (1983).
[25] G.E. Pake and T.L. Estle, *The Physical Principles of Electron Paramagnetic Resonance* (Benjamin, Reading, PA, 1973), Chap. 2.
[26] C.P. Poole, *Electron Spin Resonance* (Interscience, New York, 1967), Chap. 11.
[27] T.G. Castner, Jr., Phys. Rev. **115**, 1506 (1959).
[28] M. Stutzmann, J. Stuke, and H. Dersch, Phys. Status Solidi B **115**, 141 (1983).
[29] N. Ishii, M. Kumeda, and T. Shimizu, Solid State Commun. **41**, 143 (1982).
[30] R.A. Street, C.C. Tsai, M. Stutzmann, and J. Kakalios, Philos. Mag. B **56**, 289 (1987).